EES Catalysis

PAPER

View Article Online
View Journal | View Issue

Cite this: *EES Catal.*, 2024, 2, 1111

Catalytic upgrading of wet waste-derived carboxylic acids to sustainable aviation fuel and chemical feedstocks†

Jacob H. Miller, *[a] Mayadhin Al Abri,[a] Jim Stunkel,[a] Andrew J. Koehler,[a] Matthew R. Wiatrowski,[a] Robert L. McCormick,[b] Gina Fioroni,[b] Jon Luecke,[b] Cheyenne Paeper[a] and Martha Arellano-Treviño[a]

Received 22nd April 2024,
Accepted 11th June 2024

DOI: 10.1039/d4ey00087k

rsc.li/eescatalysis

We develop a catalytic process comprising exclusively of flow reactions for conversion of wet waste-derived volatile fatty acids to sustainable aviation fuel (SAF) and key aromatic building blocks (benzene, toluene, ethylbenzene, and xylene; BTEX). Acids are upgraded *via* sequential ketonization and either cyclization of light (C_{3-7}) ketones to BTEX and an aromatic SAF blendstock or hydrodeoxygenation of C_{8+} ketones to an alkane SAF blendstock. The enabling step investigated in this work is light ketone cyclization over H/ZSM-5, which was chosen through screening upgrading of 4-heptanone over solid acidic and basic catalysts. We then determined the reaction network of 4-heptanone upgrading by analyzing selectivity trends with conversion and concluded that the reaction should be run at full conversion. Finally, we demonstrated the entire acid upgrading process by converting commercial food waste-derived carboxylic acids to SAF blendstocks and BTEX. We blended the C_{9+} aromatic and alkane products to create one SAF blendstock and show that this mixture can be blended 50/50 with Jet A and meet all critical property standards. Techno-economic analysis and life cycle assessment show that utilizing a food waste feedstock for the process can be economically feasible with current policy incentives and reduce greenhouse gas emissions by more than 250%.

Broader context

Biomass and waste carbon resource upgrading must play a role in our decarbonized future to replace petroleum-derived fuels and chemicals used in critical functions such as aviation and materials. The U.S. Department of Energy highlighted this recently in their release of the "Clean Fuels & Products Earthshot," which aims for 100% decarbonization of aviation fuel, 50% decarbonization of maritime, rail, and off-road fuels, and 50% decarbonization of carbon-based chemicals by 2050, eliminating 650 million metric tons of CO_2 emissions annually in the USA alone. The pathway we present here addresses both vital applications, as products consist of both fuels and chemicals, and it is developed through a fundamental study of internal ketone upgrading on H/ZSM-5. The work presented in this paper shows the important role that wet waste upgrading can play in decarbonizing the aviation and chemical industries.

Introduction

The increasing scope and effects of anthropogenic climate change[1] require rapid action to decarbonize all sectors of the global economy. Two critical industries to decarbonize, recently identified by the United States Department of Energy through the "Clean Fuels & Products Earthshot," are fuels (particularly aviation fuel) and chemicals.[2] This Earthshot aims to satisfy 100% of our aviation demand with sustainable aviation fuel (SAF) and 50% of our carbon-based chemical demand with sustainable chemicals by 2050. One promising sustainable feedstock for decarbonization of these two sectors is wet waste. Infrastructure for valorization of wet waste *via* anaerobic digestion to biogas (mixtures of CH_4 and CO_2) is rapidly expanding across the United States,[3] while rapid advancements have recently been made in scaling up processes to arrest the anaerobic digestion process, forming carboxylic acids.[4–6] Wet waste is generated in the United States with energy content equivalent to 10.5 billion gallons per year aviation fuel, enough

[a] *Catalytic Carbon Transformation and Scale-Up Center, National Renewable Energy Laboratory, Golden, CO, USA. E-mail: jacob.miller@nrel.gov*
[b] *Center for Integrated Mobility Sciences, National Renewable Energy Laboratory, Golden, CO, USA*

† Electronic supplementary information (ESI) available. See DOI: https://doi.org/10.1039/d4ey00087k

to satisfy 30% of the projected 2050 SAF demand.[4,7,8] Additionally, wet-waste derived fuels can have net-negative life-cycle carbon intensities due to the avoidance of naturally-occurring emissions of CH_4, a greenhouse gas with more than 28 times the heat trapping potency of CO_2,[9] resultant from standard waste mitigation practices.[7,10] The market for benzene, toluene, ethylbenzene, and xylene (BTEX), a critical family of chemicals used for many applications such as polyethylene terephthalate, is also quite large, with greater than 150 million tons of annual production; these molecules are overwhelmingly sourced from petroleum.[11]

Valorization of carboxylic acids (also known as volatile fatty acids, or VFAs) to SAF was previously demonstrated by our group using a multi-step approach.[7] The carboxylic acids were first ketonized over ZrO_2. Then, C_{8+} ketones were hydrotreated to alkanes over Pt/Al_2O_3 to form mostly *n*-alkanes, while C_{3-7} ketones underwent aldol condensation over niobic acid followed by hydrotreatment over Pt/Al_2O_3 to form branched and cyclic alkanes. All steps were run in continuous reactors besides aldol condensation, which was performed in stirred batch reactors. We seek in this work to find a continuous process for valorization of light ketones, as continuous processes scale more effectively than batch processes.

Previous work has shown that many catalysts including $MgZrO_x$,[12] TiO_2,[13,14] ZrO_2,[14] $Mg_6Al_2O_9$,[15,16] and Cu/ZrO_2[17] can couple light ketones to form jet-range molecules. However, most work over these catalysts has been focused on methyl ketones, with Sun *et al.*[12] specifically noting that catalyst activity for coupling of internal ketones (that is, ketones with both alkyl chains possessing two or more carbon atoms) was negligible compared to methyl or cyclic ketones, with most observed internal ketone conversion occurring *via* reactions of internal ketones with methyl or cyclic ketones or aldehydes in batch reactions over $MgZrO_x$. Thus, conversion of internal ketones is a significant challenge. The light ketone feedstocks we seek to valorize in this work consist primarily of internal ketones. For example, a fermentation process under development at NREL produces purely butyric acid (ketonization product: 4-heptanone),[18–20] while light ketones derived from mixtures of VFAs such as those considered in this paper contain >70% (C mol basis) internal ketones. Zeolites, however, particularly H/ZSM-5, have been shown to convert mixtures of acids or ketones to hydrocarbons at 350–450 °C, although reactions generally form mixtures of approximately equal amounts of aromatic hydrocarbons and light (C_{1-6}) alkanes or alkenes.[21–26] Out of these mixtures, light hydrocarbons and aromatics of carbon numbers lower than eight are not well suited as SAF blendstocks, although C_{6-8} BTEX aromatics can be utilized as valuable chemical precursors.

In this work, we seek to develop a continuous catalytic process for converting 4-heptanone, a model internal ketone, to a SAF blendstock by first screening reactions over multiple solid acidic and basic catalysts. We down-select H/ZSM-5 and study the products and reaction network for 4-heptanone upgrading, showing that optimal value can be derived from the reaction by running it at full conversion. Next, we demonstrate that catalyst deactivation can be mitigated by regeneration in air and that butyric acid deactivates the catalyst much more rapidly than 4-heptanone. We then upgrade a mixture of commercial, food waste-derived carboxylic acids to aromatic and alkane SAF blendstocks and BTEX in a catalytic process that incorporates light ketone upgrading over H/ZSM-5. We combine the SAF blendstocks to create a blend which meets the minimum 8 vol% aromatic requirement for finished synthetic aviation turbine fuels.[27] Finally, we show that the 8 vol% aromatic SAF blendstock formed in this process can meet critical aviation fuel properties in a 50/50 (vol/vol) blend with Jet A and that the process makes sustainably-sourced aviation fuel and BTEX from food waste, resulting in a 268% reduction in life cycle greenhouse gas (GHG) emissions. With the inclusion of policy incentives, this approach can be economically competitive with petroleum jet fuel, demonstrating a minimum jet selling price (MJSP) of $2.30 per gal.

Experimental section

Solid acidic and basic catalysts screened for 4-heptanone upgrading included ZrO_2 (Johnson Matthey, pretreated in stagnant air at 550 °C for two hours as in our previous work[28]), TiO_2 (Alfa Aesar), niobic acid (CBMM, pretreated in stagnant air at 350 °C for 12 hours as in our previous work[7,29]), $Mg_6Al_2O_9$ (from Sigma Aldrich hydrotalcite, pretreated in stagnant air at 700 °C for 2 hours), H-beta zeolite (H/BEA; Tosoh HSZ-940HOA, Si/Al = 14), H-faujasite zeolite (H/FAU; Zeolyst CBV 720, Si/Al = 15), H-mordenite zeolite (H/MOR; Thermo Scientific, Si/Al = 10), and H/ZSM-5 zeolite (Zeolyst CBV8014, Si/Al = 40). All zeolites were received in NH_4 form and were pretreated in stagnant air for 8 hours at 550 °C to convert to proton form. H/ZSM-5 was down-selected as a light ketone upgrading catalyst (*vide infra*), and the X-ray diffractogram of it is shown in Fig. S1 (ESI†). Specific surface areas of all catalysts were measured using N_2 physisorption on a Quantachrome Instruments Quadrasorb SI (Table S2, ESI†). Precious metal catalysts supported on Al_2O_3, 3 wt% Pt/Al_2O_3 and 0.5 wt% Pd/Al_2O_3 (Johnson Matthey), were used for ketone hydrodeoxygenation and aromatics saturation, respectively. Catalysts were pelletized and sieved before use and particles with sizes between 177 and 400 μm were usually used in reactions.

4-Heptanone (98%, Sigma-Aldrich), butyric acid (≥99%, Sigma-Aldrich), and a food waste-derived mixture of carboxylic acid salts (ChainCraft, ''Mixture of short and medium chain fatty acid sodium salts'') were used as reactants in this work. ChainCraft salts were converted to proton form by mixing with hydrochloric acid (Fisher Scientific, 12.1 M; HCl : acid salt molar ratio: 1 : 1.1) in a glass beaker, vacuum filtration of the two-phase mixture using an 11 μm filter (Whatman #1), extraction of the organic layer (a translucent, brown liquid) in a separatory funnel, and spinning-band distillation to remove residual solids, resulting in a clear liquid. Carboxylic acids boiling off between 110–170 °C constituted light acids, while acids boiling between 170–240 °C constituted heavy acids.

Reactions were performed in a Dursan-coated (SilcoTek Coating Co.) stainless steel clamshell-heated packed-bed reactor described previously,[28] with all catalyst and reaction condition evaluation reactions taking place in a 4.7×10^{-3} m ID reactor and ChainCraft acid upgrading reactions taking place in a 1.0×10^{-2} m ID reactor. Gases were fed using mass flow controllers from Brooks Instruments, while liquids were combined using a high-pressure liquid chromatography (HPLC) pump from Chromtech and then vaporized in a heated inlet (200 °C). Helium (Matheson Gas, 99.999%) was used as a sweep gas. Liquid consumption was measured by placing liquid reservoirs on mass balances (Mettler Toledo) and monitoring mass changes over time. The reaction mixture was passed through a catalyst bed containing 0.1–5.0 g catalyst (pelletized, crushed, and sieved to particle sizes between 150 and 600 μm) supported by plugs of glass wool and, in 1.0×10^{-2} m ID reactors, bed packings of 1 mm untreated glass beads (BioSpec Products) held in place by a plug of glass wool (Ohio Valley Specialty). Temperature was monitored *via* a concentric thermocouple (Omega) placed inside the catalyst bed. Reactor effluents were condensed in a liquid-cooled heat exchanger (2 °C) and collected periodically (every 4–24 hours) from a knockout pot. Gaseous products were monitored inline using an Agilent 6890 gas chromatograph equipped with a thermal conductivity detector, while liquid products collected from the knockout pot were quantified using a separate Agilent 7890A gas chromatograph equipped with a 5975C mass spectrometer and a PolyARC quantitative carbon detector (Activated Research Company). The reactor system is equipped with robust process monitoring which tracks system pressure, temperature, and possible leakages and shuts the system down in the case of deviations from expected conditions, ensuring operator safety.

Carbon balances (CB) were measured according to the formula:

$$\mathrm{CB} = \frac{\sum_i C_{n,i}\dot{n}_i}{\sum_i C_{n,i}\dot{n}_{i,0}} \quad (1)$$

Here, $C_{n,i}$ is the carbon number of species i, n_i is the effluent molar flowrate of species i, and $n_{i,0}$ is the influent molar flowrate of species i. Carbon balances were usually closed within 80%, and closure was only obtained after *ca.* 20 hours on stream due to the low flowrates and large reactor sizes; data are only reported from samples with adequate carbon closure. Yields of each product i (Y_i) were calculated on a carbon basis according to the formula:

$$Y_i = \frac{C_{n,i}\dot{n}_i}{\sum_j C_{n,j}\dot{n}_{j,0}} \quad (2)$$

Conversion of a reactant j (X_j) when the reactant was observed in the reactor effluent was calculated using:

$$X_j = \frac{\sum_i C_{n,i}\dot{n}_i}{C_{n,j}\dot{n}_{j,0}} \quad (3)$$

Conversion was reported as complete (100%) when no reactant was present in the effluent. Selectivities of each product i (S_i) were calculated by evaluating:

$$S_i = \frac{Y_i}{X_j} \quad (4)$$

In (1)–(4), products are delineated by the subscript i, while reactants are delineated with the subscript j. Existence of interphase and intraparticle heat and mass transport limitations was evaluated for 4-heptanone reactions over H/ZSM-5 using criteria developed by Mears[30] and Weisz and Prater,[31] respectively (Section S1, ESI†). The calculations confirm that our conditions did not engender significant interphase mass or thermal gradients or interparticle thermal gradients. We did predict the existence of significant intraparticle mass transport limitations, but these are known to affect reactions of similarly-sized molecules in zeolites at comparable temperatures.[32,33]

Heteroatom impurity content of fuels, intermediates, and catalysts was determined *via* inductively couple plasma optical emission spectroscopy (ICP-OES) as detailed in Section S2 (ESI†). Quantification of halogen and nitrogen content (*via* chemiluminescence) was performed by Hazen Research, Inc. A thermal regeneration procedure for spent H/ZSM-5 was developed *via* thermogravimetric analysis (TGA) using a Setaram Setsys Evolution instrument, with details described in Section S2 (ESI†).

Fuel properties of the final 50/50 (vol/vol) mixture of SAF blendstock and Jet A were measured using ASTM standard methods. These properties include distillation (*via* simulated distillation), flash point, viscosity at −20 and −40 °C, density at 15 °C, surface tension at 20 °C, freezing point, lower heating value (*via* higher heating value and hydrogen weight fraction), and cetane number. Details of the ASTM methods used for these measurements are described in Section S2 (ESI†). The Jet A sample was obtained from a petroleum refiner and has properties that are in the typical range for jet fuel based on the CRC World Fuel Sampling Program survey (Table S5, ESI†).[34]

We evaluated the economic feasibility and sustainability of the described process using techno-economic analysis (TEA) and life cycle assessment (LCA), respectively, to assess suitability for commercialization. First, we developed a process model in Aspen Plus representing a full-scale (250 wet ton per day) commercial facility producing fuels and chemicals from food waste. VFAs were produced from food waste *via* arrested anaerobic digestion, isolated *via* solvent recovery over a pertractive membrane, and separated into light (C_2–C_4) and heavy (C_5–C_8) fractions, which were upgraded in two parallel processing trains. The first train used a ketonization reaction followed by cyclization to upgrade light VFAs (producing SAF, BTEX, and naphtha) while the second train used ketonization followed by hydrodeoxygenation to produce SAF from heavy VFAs. A process flow diagram is shown in Scheme 1, and additional modeling details are provided in the ESI† (Section S3). The mass and energy balances generated from the process model were used to

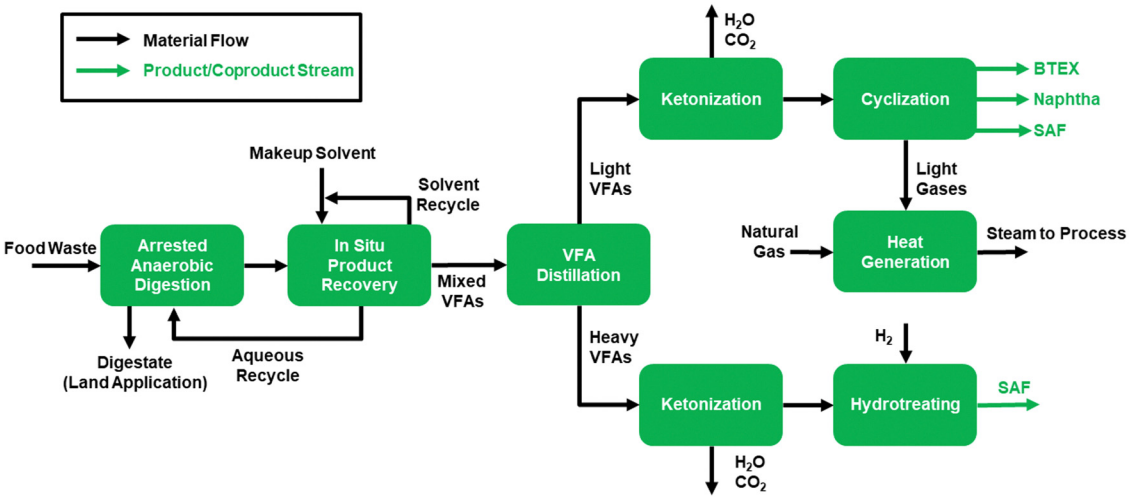

Scheme 1 Process flow diagram for the TEA and LCA process model.

inform a discounted cash flow TEA and an LCA focusing on GHG impact.

The TEA approach is consistent with our previously published studies[10,35] and uses a discounted cash flow rate-of-return (DCFROR) model to determine the minimum jet selling price (MJSP) required to obtain a net present value of zero for the plant while supporting a 10% internal rate of return. Baseline equipment costs were originally sourced from vendor quotes or generated using Aspen Capital Cost Estimator[36] and were adjusted from the original basis using scaling factors. The details of these equipment designs have been published previously.[7,10,35,37,38] Once equipment costs were determined, direct and indirect overhead cost factors were applied to determine a feasibility-level estimate of fixed capital investment (FCI) in 2020 US dollars. These factors are shown in Table S7 (ESI†) along with a summary of capital expenditures for the facility.

Variable operating expenses were calculated based on raw material and utility rates from the process model, while fixed costs (labor, maintenance, insurance, and local taxes, listed in Table S8, ESI†) are based on factors from prior works and adjusted based on plant scale.[38] Financial assumptions used in this analysis are shown in Table S9 (ESI†), which are based on a mature nth plant and consistent with prior published works. Policy incentives based on the modeled fuel carbon intensity (CI) were also included as an optional sensitivity study and are described in Table S10 (ESI†). The FCI, operating expenses, fixed costs, and revenues from co-products and policy incentives were used in the DCFROR analysis to assess the MJSP of the envisioned facility.

The cradle-to-gate LCA focused on estimating the greenhouse gas emissions of the process. The functional unit used was 1 MJ of total fuel (including both naphtha and SAF); BTEX chemicals produced were treated as a co-product using the displacement method. The life cycle inventory (LCI) was generated from the process model and assessed using CI values from the Greenhouse Gases, Regulated Emissions, and Energy Use in Transportation (GREET) model published by Argonne National Laboratory (CI values for some inputs were obtained from other sources as necessary). The LCA on GHG emissions for the process is summarized in Table S11 (ESI†). Environmental justice aspects of this research and its envisioned application were also evaluated using the JUST-R metrics recently developed by Dutta *et al.*[39] As a part of the JUST-R assessment, life cycle water consumption for the process was also estimated using the same methodology as GHG emissions (Table S12, ESI†).

Results and discussion

Catalyst screening for packed-bed reactor 4-heptanone upgrading

We screened reactions of model ketone 4-heptanone to identify a robust catalytic pathway for light ($C_{<8}$) ketone upgrading to a SAF blendstock using conventional acidic or basic catalysts. 4-Heptanone is a useful model compound because it is an interior ketone, not possessing a methyl group with easy-to-activate C–H bonds in the position adjacent to the ketonic carbon. We screened vapor-phase upgrading of 4-heptanone in a packed-bed reactor at a uniform set of conditions (T = 300–425 °C, WHSV = 1 h^{-1}, 10 vol% in flowing He) over eight oxide (ZrO_2, TiO_2, Nb_2O_5, MgAlO) or zeolite (H/ZSM-5, H/BEA, H/FAU, H/MOR) catalysts. Special attention was given to yields of molecules in the jet range (C_{9+}) over each catalyst. Fig. 1 shows the overall product and C_{9+} yields during 4-heptanone conversion over all catalysts at 350 °C, a representative condition. The figure shows that conversion (100%) and yield of C_{9+} products (29%) is the highest by far over H/ZSM-5. Significantly, conversion and C_{9+} yield over any other catalyst did not reach this level at any tested condition. Additionally, the Si/Al ratio of the H/BEA, H/FAU, and H/MOR zeolites examined in this work was lower than H/ZSM-5 (equivalently, Brønsted acid density of all other zeolites was higher than that of H/ZSM-5), meaning

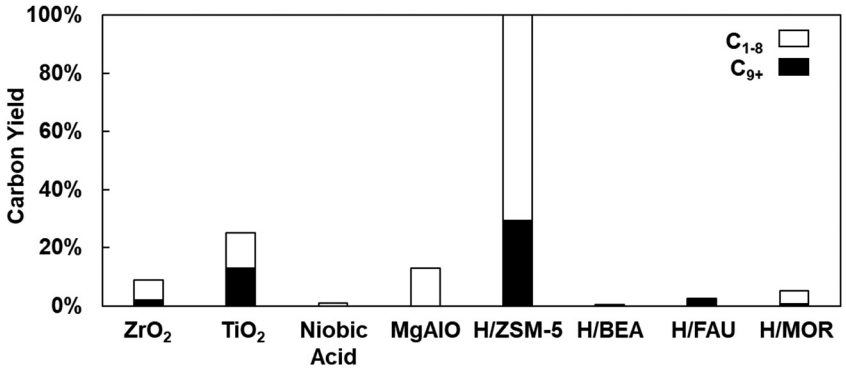

Fig. 1 Screening catalysts for 4-heptanone upgrading. C_{9+} products are desired for jet applications. Reaction conditions: T: 350 °C, P_{Total} = 150 kPa, $P_{4\text{-Heptanone}}$ = 15 kPa, balance He (30 sccm), WHSV = 1 h^{-1}, $m_{catalyst}$ = 1 g.

that the higher conversions achieved over H/ZSM-5 are not simply attributable this catalyst having higher acid site density than the other three zeolites. The low conversions over most catalysts shown in Fig. 1 reinforce that activation and upgrading of interior ketones is not nearly as facile as activation and upgrading of methyl ketones over catalysts demonstrated to be robust at the latter reaction (*e.g.*, MgAlO, TiO_2, ZrO_2).[12,13,15–17] We down-selected H/ZSM-5 for further study as a light ketone upgrading catalyst.

Products of 4-heptanone upgrading over H/ZSM-5 and catalyst deactivation

We next monitored conversion of 4-heptanone over H/ZSM-5 at 350 °C over a substantial time on stream (>100 hours) to better understand the products formed at full conversion and determine whether substantial deactivation occurs. Fig. 2A illustrates conversion of 4-heptanone with time on stream over 115 hours. Substantial deactivation is apparent, as conversion drops from 100% up to 67 hours to 69% at 115 hours. We stress and will discuss in more detail below that the catalyst bed is continuously deactivating over the course of this reaction, but that the bed in this experiment (WHSV = 1 h^{-1}) is "overfilled" initially, causing 4-heptanone conversion to remain complete over the first 67 hours on stream before dropping.

Fig. 2B shows the product distribution observed at full 4-heptanone conversion averaged over the first five data points shown in Fig. 2A. Carbon number distribution of the products is bimodal—C_{7-13} products are primarily aromatics, with C_8 species having the highest selectivity (23%), while C_{1-6} products are primarily alkanes, with C_4 molecules having the highest selectivity (16%). As noted earlier, selectivity to C_{9+} jet-range products is substantial (28% over these samples). Furthermore, selectivity to valuable BTEX products is also high (29%), further hinting at the value of this upgrading pathway (*vide infra*). Since most C_{7+} products formed in this process are cyclic, we refer to this process as "cyclization".

Although aromatics are currently a necessary constituent of aviation fuel, eventual elimination of these compounds to decrease formation of soot in the upper atmosphere, among other benefits, is desirable. Soot formation is accelerated by combustion of aromatic rings.[40] We eliminated the aromatic rings of the liquid 4-heptanone upgrading products by saturating them over Pd/Al_2O_3 in the presence of H_2 (T = 200 °C, P_{H_2} = 3500 kPa, WHSV = 0.24 h^{-1}). The results of this

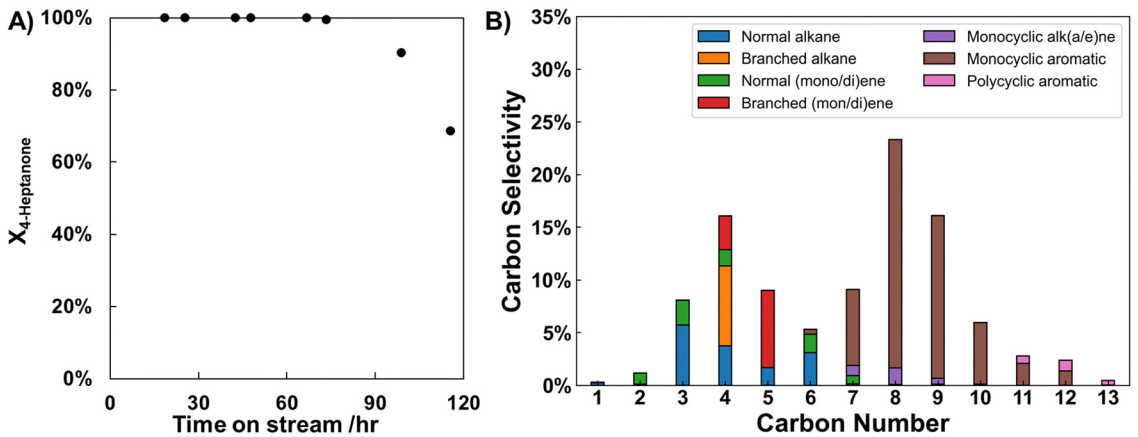

Fig. 2 (A) 4-Heptanone conversion ($X_{4\text{-heptanone}}$) over time and (B) product selectivities at full conversion in 4-heptanone upgrading over H/ZSM-5 (Si/Al = 40). Reaction conditions: T = 350 °C, P_{Total} = 140 kPa, $P_{4\text{-Heptanone}}$ = 14 kPa, balance He (30 sccm), WHSV = 1 h^{-1}, $m_{H/ZSM\text{-}5}$ = 1 g. Product selectivities are cumulative selectivities from 0–73 hours on stream.

demonstration, shown in Fig. S2 (ESI†), show that saturation of all molecules is facile and forms primarily cycloalkanes. Thus, products of light ketone upgrading over H/ZSM-5 can also be utilized in future aromatics-free SAF applications.

Reaction network of 4-heptanone upgrading shows accessing a higher carbon number range product is not possible

The data in the last section show that upgrading model light ketone 4-heptanone over H/ZSM-5 forms a product somewhat compatible with sustainable aviation fuel applications. An ideal product mixture, however, would have carbon numbers centered around eleven, the center of the carbon number distribution of aviation fuel.[41] In concept, 4-heptanone could form products of carbon numbers near eleven *via* several activation pathways. Scheme 2 shows four possible pathways for initial reactions of 4-heptanone over acid catalysts: (i) dehydration to heptadiene or methylcyclohexene (the latter with accompanying cyclization), (ii) cracking to propylene and a C_4 oxygenated fragment, (iii) C–C bond formation between propylene and a C_7 to form C_{10} species such as 4-propyl 2-heptene, and (iv) aldol condensation to form C_{14} enones. The latter two pathways form products with carbon numbers useful for SAF applications. Although 4-heptanone upgrading at full conversion does not form substantial amounts of products with carbon numbers higher than nine, it is conceivable that larger species could form initially and undergo subsequent consumption through C–C bond scission reactions. If this was the case, these products could be collected for SAF applications through catalyst alteration or process modification (*e.g.*, running the reaction at sub-complete conversion with a recycle loop).

We assessed the possibility that running 4-heptanone upgrading at sub-complete conversion could create products more applicable to SAF than the products formed at complete conversion by performing first-rank delplot analysis, which entails examining selectivities of major products as a function of reactant conversion.[42,43] In this formalism, products with finite selectivity at zero conversion are proven to be primary products (forming *via* reactions involving the reactant), while products with zero selectivity at this conversion are secondary (forming *via* reactions involving primary products) or higher-rank products. Additionally, we apply Wojciechowski's criteria[44,45] to first-rank delplots to determine product stability. Products are unstable (consumed in subsequent reactions) if selectivity decreases with increasing conversion, while they are stable if selectivity remains constant or increases with increasing conversion. This technique has been utilized to analyze a variety of complex reaction networks.[46–51] Two aspects of 4-heptanone upgrading over H-ZSM/5 differentiate it from idealized systems for delplot analysis and are worth acknowledging. First, Movick *et al.*[52] recently illustrated that the delplot technique cannot capture successive steps which occur before a reactive species desorbs from a catalyst surface. Since diffusion limitations inside H/ZSM-5 are significant, some reaction steps may not be observable. Additionally, if active sites on H/ZSM-5 are not uniform and catalyst deactivation (shown in Fig. 2A) effects some active sites more than others, modulation of conversion *via* catalyst deactivation is not equivalent to modulation *via* changing catalyst space velocity. In Fig. 3, we plot product selectivities as a function of conversion over seven different reactions; initial conversions during these reactions vary from ~20% to 100%. Since product selectivities follow the same trends regardless of initial conversion, we conclude that deactivation of active sites on H/ZSM-5 during ketone upgrading is non-selective,[53,54] meaning that product selectivity and conversion act as descriptors of reaction network progress regardless of catalyst deactivation. Thus, we can apply Wojciechowski's criteria to first-rank delplots to analyze the reaction network of 4-heptanone upgrading over H/ZSM-5 while acknowledging one limitation: it is possible that some reactions occurring in the catalyst pores may form products which are rapidly consumed in subsequent steps and are undetectable.

Fig. 3 shows first-rank delplots of several significant products categories: (A) dehydration products methylcyclohexene and heptadiene (lumped as they have the same molecular formula, C_7H_{12}), (B) C_{7-9} aromatics (toluene highlighted in orange), (C) C_{3-5} alkenes (propylene highlighted in orange), and (D) C_{3-5} alkanes. These species were specifically chosen because they cumulatively comprise the majority (52–86%) of carbon selectivity at all conversions. Analysis of the plots in Fig. 3 and other first-rank delplots allows us to identify which proposed 4-heptanone upgrading pathways in Scheme 2 are occurring. Fig. 3A and C show unambiguously that two of the primary 4-heptanone reaction pathways shown in Scheme 2, dehydration (3A) and cracking (3C), do occur, as the selectivities of C_7H_{12} species and propylene are finite at zero 4-heptanone conversion (*ca.* 30% and 15%). Furthermore, the

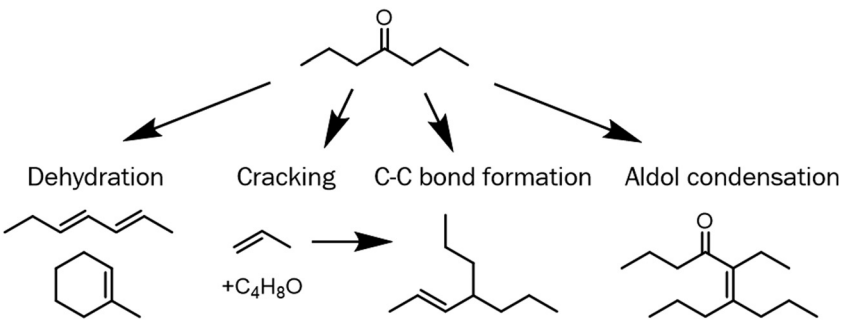

Scheme 2 Overview of possible primary pathways in 4-heptanone conversion over H/ZSM-5.

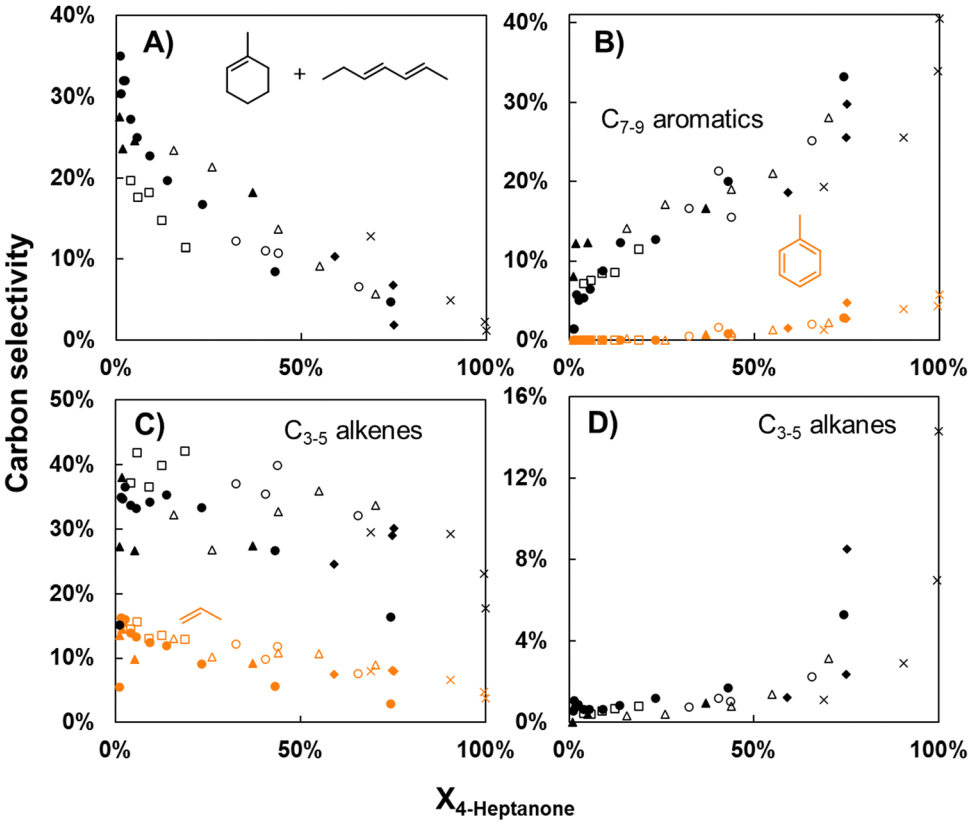

Fig. 3 Product selectivities (A: methylcyclohexene and heptadiene; B: C_{7-9} aromatics; C: C_{3-5} alkenes, and D: C_{3-5} alkanes) plotted as a function of conversion in 4-heptanone upgrading over H/ZSM-5 (Si/Al = 40) over seven packed-bed reactions run at varied space velocities. Reaction conditions: T: 350 °C, P_{Total} = 130–170 kPa, $P_{4\text{-Heptanone}}$ = 13–17 kPa, balance He (30 sccm), WHSV = 1–10 h^{-1}, $m_{H/ZSM\text{-}5}$ = 0.1–1 g, selectivities measured between 18–165 hours on stream. Conversion was modulated *via* catalyst deactivation with time on stream. Different symbols correspond to different experiments. Exemplary species (also included in each total selectivity) are plotted in orange in B (toluene) and C (propylene).

selectivity of these species declines with increasing conversion, showing that both C_7H_{12} molecules and propylene are unstable products consumed in subsequent reactions. 4-Propyl 3-heptene, the putative product of C–C bond formation between propylene and either 4-heptanone or a C_7H_{12} species shown in Scheme 2, forms with low selectivity—around 3% at $X_{4\text{-Heptanone}}$ = 1%—and is consumed rapidly, with selectivity dropping to 0% past 20% 4-heptanone conversion (data not shown in Fig. 3). Thus, this pathway is occurring, but it is not significant. Finally, no C_{14} enones are observed at any conversion, showing that the aldol condensation pathway either does not occur or forms intermediates that are too diffusionally constrained to exit the catalyst intact.

Fig. 3 also shows major products of the subsequent reactions that consume primary 4-heptanone reaction products. C_{7-9} aromatics (Fig. 3B) have close to zero initial selectivity, but this quantity monotonically increases to 35–40% at full 4-heptanone conversion. Similarly, the selectivity of C_{3-5} alkanes at zero 4-heptanone conversion is close to zero and increases to ~10% at full 4-heptanone conversion. We identify C_{7-9} aromatics and C_{3-5} alkanes as stable secondary products based on this analysis. Since formation of these secondary products depends only on the presence of primary products and not 4-heptanone, it would be expected that they would continue to form even in the absence of 4-heptanone. We show that this is the case in Fig. S3 (ESI†), where selectivity of the species lumps in Fig. 3 is plotted against time on stream during a reaction occurring at 100% 4-heptanone conversion. Despite the fact that 4-heptanone conversion is full, the selectivities of these products evolve with time on stream and display trends which show that the catalyst bed is deactivating. Data points recorded at lower times on stream are thus considered to be at higher "conversion." This quantity can also be understood as a lower residence time per active site, as the number of active sites is postulated to decrease with increasing time on stream. Significantly, selectivity of C_7H_{12} products and C_{3-5} alkenes decreases (from 1.2% to 0.4% and 18% to 3%, respectively) as residence time per active site increases (time on stream decreases), while selectivity of C_{7-9} aromatics and C_{3-5} alkanes increases (from 40% to 50% and 14% to 33%, respectively) as time on stream decreases from 65 to 15 hours.

We assimilate the data from application of Wojciechowski's criteria to first-rank delplots to formulate a proposed reaction network for 4-heptanone upgrading over H/ZSM-5 (Scheme 3). Many steps in the reaction network including the hydrogen and alkyl transfer reactions between species and deactivation *via* polyaromatics formation are identical to those seen during methanol upgrading over zeolites as illustrated by Bhan and

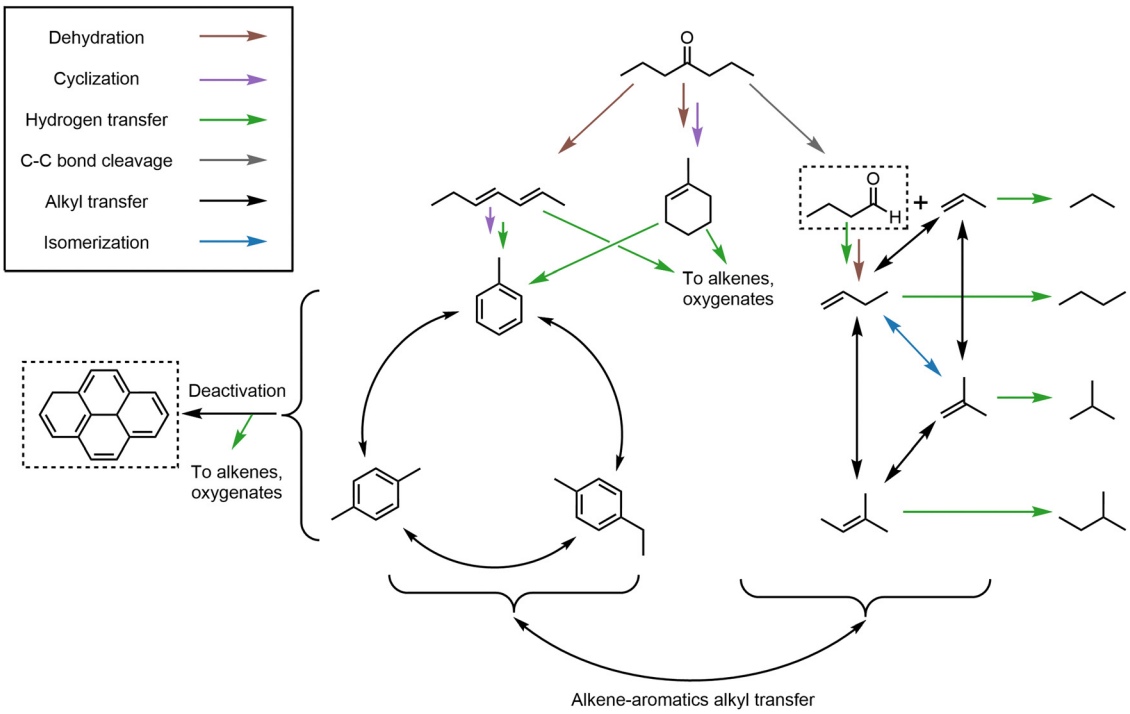

Scheme 3 Proposed reaction pathways of 4-heptanone over H-ZSM-5. Species outlined in dashed rectangles are not observed in the reactor effluent. Species shown are intended to symbolize groups of isomers with a given molecular formula. Double arrows represent multiple steps.

colleagues.[53,55,56] The reaction network provides a plausible explanation for major carbon fluxes in 4-heptanone upgrading. We propose that initial reaction of 4-heptanone occurs *via* dehydration and formation of a C_7H_{12} species (heptadiene or methylcyclohexene, only one representative isomer of each is shown) or C–C bond scission to form propylene and a C_4H_8O species (not observed in the reactor effluent). These C_7H_{12} species act as precursors to the pool of aromatic products primarily of carbon number 7–9, as shown in Scheme 3. The hydrogen atoms formed in the aromatization process are proposed to be transferred to oxygenate intermediates or alkenes, as indicated by the green arrows in the scheme. The aromatic molecule with the same carbon number as these C_7H_{12} species is toluene, but Fig. 3B shows that toluene makes up at most 15% of the total C_{7-9} aromatics species and that it is a secondary, stable product. This suggests that (i) toluene is not formed, desorbed from the zeolite, readsorbed, then subsequently alkylated to higher carbon number aromatics in significant amounts and (ii) carbon chain growth (and cleavage) of aromatic precursor species *via* alkyl fragments in the zeolite is facile.

We postulate that a pool of light alkane and alkene species forms in parallel to the aromatics pool. Initial fluxes to this pool likely arise from primary cracking of 4-heptanone and subsequent dehydration of oxygen-containing fragments, which both form alkene species. These alkene species interconvert *via* isomerization and alkyl exchange both within the alkene pool and with the aromatic pool. As discussed above, alkenes are not terminal products—they are hydrogenated to corresponding alkanes *via* hydrogen transfer, with significant hydrogen flux arising from aromatization reactions. Another source of hydrogen for alkene saturation is growth of polycyclic aromatics from sources within the aromatics pool. This reaction forms carbonaceous coke (not observed in reactor effluents), which we propose causes catalyst deactivation. We will show how this coke can be removed to regenerate the catalyst below.

Analysis of the 4-heptanone upgrading reaction network discussed in this section shows that no alteration of system conversion would make significant amounts of products more suited for SAF applications (carbon numbers closer to 11) than the products formed at full reactant conversion, as the major products formed at sub-complete conversion have similar carbon numbers to those formed at complete conversion. Fig. S4 (ESI†) succinctly illustrates this trend, showing that the average carbon number of products formed at all 4-heptanone conversions is close to seven. We specifically confirmed that primary 4-heptanone reaction pathways hypothesized to form C_{14} (aldol condensation) or C_{10} (C–C bond formation) are either not observed (aldol condensation) or insignificant (C–C bond formation). This evidence indicates that the most efficient catalytic upgrading configuration for model ketone 4-heptanone over H/ZSM-5 is running at complete conversion.

H/ZSM-5 can be regenerated in air to recover ketone upgrading performance

We developed a thermal regeneration procedure for spent H/ZSM-5 in air to remove accumulated polyaromatic carbon from the catalyst. Fig. S5 (ESI†) shows results of thermogravimetric analysis (TGA) performed in air of two H/ZSM-5 catalysts

previously used in 4-heptanone upgrading reactions. Fig. S5A (ESI†) shows that ramping the temperature to 800 °C results in combustion of *ca.* 13% of sample weight, all of the accumulated polyaromatic species. Hoff *et al.*[57] found that treatments at this temperature result in loss of acid sites driven by dealumination, so regeneration at 800 °C is not desirable. Accordingly, we performed a similar regeneration (Fig. S5B, ESI†) while holding the catalyst temperature at 550 °C instead of ramping further and observed the same amount of mass loss (*ca.* ∼13%) due to combusted coke. Thus, we chose to regenerate at 550 °C, as was done by Wang *et al.*[25] and Cao *et al.*[21] for regeneration of H/ZSM-5 used in upgrading of carboxylic acids to hydrocarbons.

We tested our regeneration protocol by running 4-heptanone upgrading at partial conversion, deactivating the catalyst for ∼75 hours, removing the catalyst from the reactor and regenerating it at 550 °C in a muffle furnace in stagnant air, and repeating the procedure two more times. Fig. 4 shows 4-heptanone conversion over time during these repeated regeneration experiments. Significantly, the once- and twice-regenerated catalysts have very similar deactivation trends over time, with the twice-regenerated catalyst even achieving higher conversions at low (<40 hours) times on stream compared to the once-regenerated catalyst. Conversion of 4-heptanone over time is likewise indistinguishable within error between the regenerated and fresh catalysts after 40 hours on stream. Conversion at low times on stream (<40 hours) is higher over the fresh catalyst than the regenerated catalysts (by *ca.* 10–30%), indicating that a portion of active sites on H/ZSM-5 are irreversibly deactivated at reaction conditions. However, the consistency in deactivation over time between the two catalyst regenerations implies that H/ZSM-5 can be repeatedly regenerated by burning off accumulated polyaromatic carbon species.

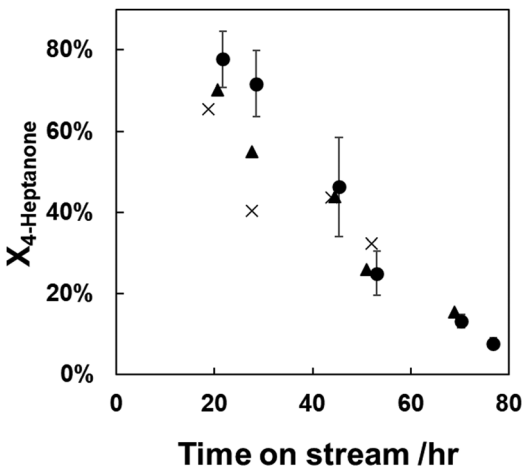

Fig. 4 Deactivation trends in 4-heptanone upgrading over H/ZSM-5 during repeated experiments with intervening catalyst regenerations. Reaction conditions: *T*: 350 °C, P_{Tot} = 140–160 kPa, WHSV = 3.1–3.6 h^{-1}, $m_{catalyst}$ = 0.27–0.31 g. ●: fresh catalyst (0.30 g); ×: once-regenerated catalyst (0.31 g); ▲: twice-regenerated catalyst (0.27 g). Error bars are standard deviations of three independent runs on fresh catalysts.

Butyric acid can be directly upgraded over H/ZSM-5 but deactivates the catalyst much more rapidly than 4-heptanone

Brønsted acid sites can facilitate ketonization reactions[58] along with the pathways discussed above. In concept, then, acids can be fed over H/ZSM-5 and generate the product slate as ketones. We fed butyric acid, the precursor to 4-heptanone, over H/ZSM-5 at comparable influent carbon flowrates to the 4-heptanone upgrading reactions discussed above and contrasted the yields of liquid products obtained over time. Fig. 5 compares these yields between 4-heptanone and butyric acid reactants over time. The contrast is stark; C_{7+} hydrocarbon yields obtained during butyric acid upgrading fall below 1% within less than 40 hours on stream, whereas yields of these products (*ca.* 50%) reflect full 4-heptanone conversion up to 80 hours on stream. Thus, although butyric acid can be upgraded to the same products as 4-heptanone over H/ZSM-5, it causes rapid catalyst deactivation. Additionally, ketonization catalysts such as ZrO_2 and TiO_2 are much more resilient to deactivation.[7,24,59,60] It follows that one-step conversion of butyric acid to hydrocarbon upgrading products over H/ZSM-5 is impractical. Wang *et al.*,[25] Cao *et al.*,[21] and Fufachev *et al.*[24] reported similar conclusions when comparing reactions of ketones and carboxylic acids over H/ZSM-5, and all of these conclusions are in line with Zhang *et al.*'s[61] observation that deactivation rates during oxygenate conversion reactions over zeolites increase with decreasing H/C_{eff} ratio, defined as:

$$\frac{H}{C_{eff}} = \frac{H - 2O}{C} \quad (5)$$

Here, H, O, and C are the numbers of hydrogen, oxygen, and carbon atoms in a reactant's molecular formula. The H/C_{eff} value of 4-heptanone is ∼1.7, while the H/C_{eff} value of butyric acid is 1, roughly 40% lower. Since the oxygen content of butyric acid is significantly higher than that of 4-heptanone, ketonizing butyric acid over a separate catalyst (*e.g.*, ZrO_2 or

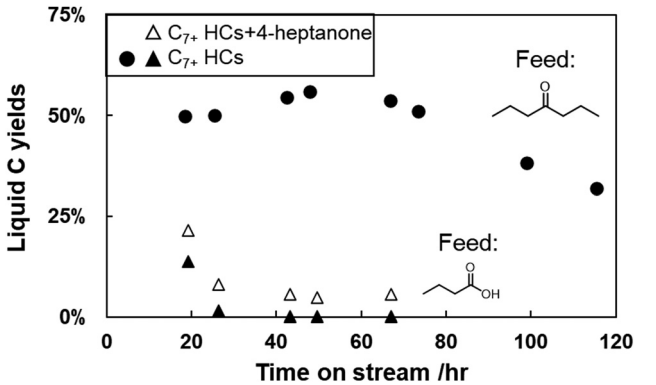

Fig. 5 Comparison of H/ZSM-5 deactivation with time on stream during reactions of 4-heptanone (circles) and butyric acid (triangles) at comparable influent carbon flowrates (4-heptanone: 0.058 mol_C $g_{H/ZSM-5}$ h^{-1}; butyric acid: 0.053 mol_C $g_{H/ZSM-5}$ h^{-1}). Reaction conditions: *T*: 350 °C, P_{Total} = 140 kPa, $P_{4\text{-Heptanone}}$ = 14 kPa or $P_{Butyric\ acid}$ = 23 kPa, balance He (30 sccm), WHSV = 0.95 (4-heptanone) or 1.16 (butyric acid) h^{-1}, $m_{H/ZSM-5}$ = 1 g.

TiO_2) before upgrading it over H/ZSM-5 is an advantageous strategy to extend catalyst lifetime.

Upgrading of commercial, bio-derived carboxylic acids to SAF blendstocks and BTEX

We obtained carboxylic acid salts derived from food waste from ChainCraft's commercial-scale production process, then upgraded them as shown in Fig. 6A. First, the acid salts were converted to proton form by mixing with HCl, followed by separation *via* spinning-band distillation into light (primarily C_4) and heavy (primarily C_6) acid fractions, with carbon number distributions of each fraction displayed in Fig. 6B and C. Both fractions of carboxylic acids were then ketonized separately over ZrO_2 in a vapor-phase packed-bed reactor (T = 380 °C, P_{Total} = 160 kPa, WHSV = 0.6 h^{-1}, 9 sccm helium sweep gas, m_{ZrO_2} = 5 g). We note that the acids were ketonized separately to maximize the yield of jet-range (primarily C_{9+}) ketones, which our prior work has shown are formed in highest concentrations from ketonization of exclusively C_{5+} carboxylic acids.[10] Carbon number distribution of ketones formed is shown in Fig. 6D and E for light and heavy VFA reactants, respectively. The primarily C_{5-7} light ketone stream was then upgraded over H/ZSM-5 using the conditions developed above (T = 350 °C, P_{Total} = 180 kPa, WHSV = 1 h^{-1}, 120 sccm He sweep gas, $m_{H/ZSM-5}$ = 4 g), with the final product speciation and carbon number distribution shown in Fig. 6F. The heavier ketone stream was hydrotreated over Pt/Al_2O_3 using conditions developed in our prior work[7] (T = 345 °C, P_{Total} = 3500 kPa, WHSV = 3.6 h^{-1}, 265 sccm H_2, m_{Pt/Al_2O_3} = 1 g); carbon number distribution of the primarily *n*-alkane final product is shown in Fig. 6G. All reactions were run at full reactant conversion.

Fig. 6F shows that BTEX aromatics have particularly high selectivity. The yields of each one of these species are shown in Fig. S6 (ESI†); the majority of BTEX products formed are toluene (36 carbon% of BTEX carbon yield) and *p*-xylene (40%), with the rest comprising benzene, ethylbenzene, and *o*-xylene. Heteroatom (N, halogens, Al, B, Ca, Co, Cr, Fe, K, Li, Mg, Mn, Na, Ni, P, S, Sr, and Zn) content of process inputs, liquids formed at all stages of the process, and some catalysts were also measured (Table S6, ESI†). Both liquid hydrocarbon product streams (the C_{6-13} BTEX and aromatic SAF blendstock formed from light VFAs and the C_{7-13} alkane blendstock formed from the heavy VFAs) had heteroatom contents below the detection limit (typically 2 ppm), with the exception of Na (3 ppm) in the alkane blendstock. This residual Na from the mixed acid salt feedstock could likely be dramatically lowered in an intensified process. The tiered screening process for SAF blendstocks only requires that the Na level be reported. However, for Fast Track screening (allowing blending up to 10 vol%), Na is limited to no more than 0.1 ppm.[27] The generally low contaminant levels make the fuels feasible SAF blendstocks.[62]

Particularly relevant is the undetectable amount of N contamination in these blendstocks. The food waste feedstock for the process contains >6000 ppm N (Fig. S7, ESI†), the biological arrested methanogenesis process reduces this number 60-fold (to 101 ppm), and the subsequent thermochemical upgrading steps render final products containing <1 ppm N. Similar to the situation for Na, the tiered screening process for

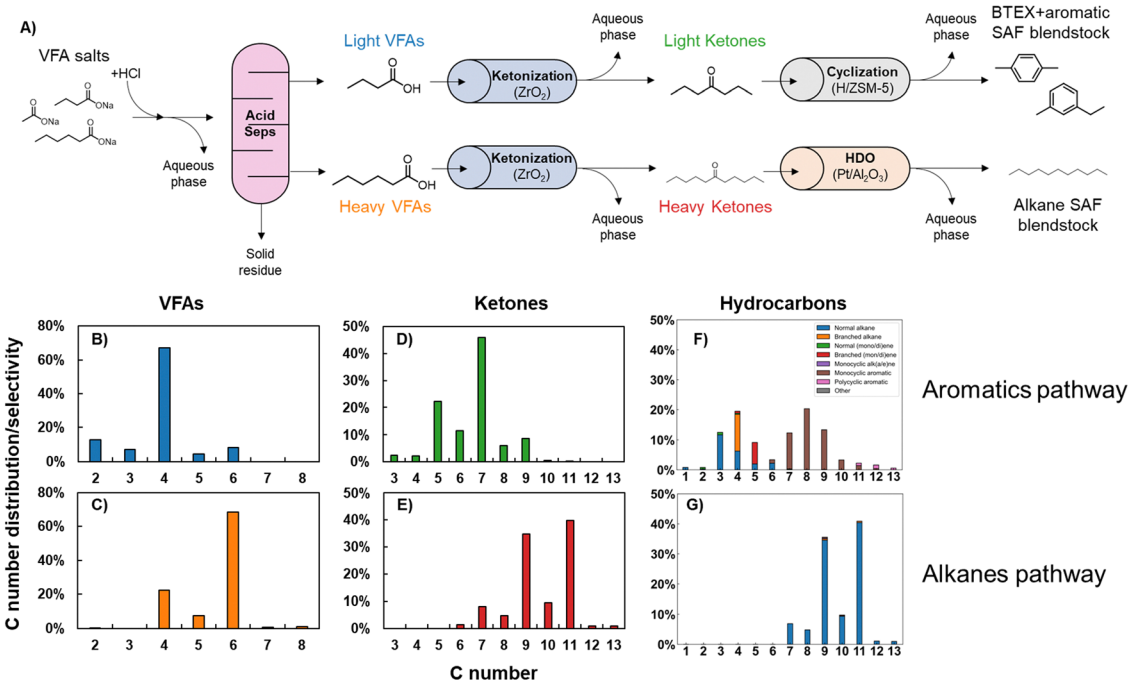

Fig. 6 Summary of VFA salts upgrading process and results. (A) Schematic of process; (B) and (C) carbon chain length distribution of light and heavy VFA streams (respectively); (D) and (E) carbon chain length distribution of ketones from light and heavy VFA streams (respectively); (F) and (G) carbon number distribution and speciation of light VFA-derived aromatics and light hydrocarbons and heavy VFA-derived alkanes (respectively).

SAF blendstocks only requires that N level be reported, but N must be less than 2 ppm for Fast Track screening.[27] Here the biological conversion step and subsequent separation to convert food waste to VFA salts successfully eliminates most N contamination without the need for a specific denitrogenation process. By contrast, upgraded oils from hydrothermal liquefaction, another promising wet waste upgrading procedure, commonly contain *ca.* 1 wt% N without deployment of a dedicated deep denitrogenation step.[63] Overall mass fluxes for the upgrading process are shown in Fig. S8 (ESI†). The significant flux to side products, particularly residual solids, shows that overall yields would increase if the upstream separation steps were optimized and the process were integrated.

Alkane and aromatic products can be blended up to 50% in Jet A while meeting critical fuel property standards

A SAF blendstock containing alkanes from heavy VFAs (92 vol%) and primarily aromatics from light VFAs (8 vol%) was created and mixed with a commercial Jet A sample (50/50 vol/vol). The aromatic blendstock content was chosen to be 8 vol% to match the minimum aromatics content required for seal swelling in aviation fuels containing synthetic (*e.g.* sustainable) compliants.[27] Both bio-derived blendstocks were altered slightly from the liquid products collected in the previous section. Heptane and BTEX aromatics were separated from the alkane and aromatic blendstocks, respectively, by distillation, to better conform to aviation-range boiling point curves and flash point limitations and route C_{6-8} aromatics to valuable BTEX applications. The final distillations led to an alkane blendstock with a flash point of 39.9 °C and freezing point of −41.2 °C. The flash point of the aromatic blendstock was 52.2 °C and freezing point was below −70 °C.

Fig. 7A shows the carbon number distribution and molecular functionality of the 8 vol% aromatic mixed SAF blendstock, while Fig. 7B shows that the boiling point range of the 50/50 blend falls within the typical range of aviation fuel properties as assessed by the CRC World Fuel Sampling Program.[34] This blend also meets the distillation slope criteria of T50–T10 > 15 °C (29.5 °C) and T90–T10 > 40 °C (74.9 °C) and the boiling point criteria of T10 < 205 °C (163.5 °C) and final boiling point <300 °C (271.2 °C).[64] Important physical and combustion properties of the fuel blend are shown in comparison to ASTM-approved ranges or limits (light blue) and typical Jet A ranges (dark blue) from the CRC sampling program in Fig. 7C. Flash point, freezing point, lower heating value (LHV), density, and viscosity all meet the specification requirements for jet fuels containing synthetic components and fall within the historical range for jet fuels. Cetane number is in the acceptable range and surface tension falls within the historical range of conventional Jet A.[62]

Thus, fuel property analysis shows that a 50/50 blend of the SAF blendstock developed in this work and Jet A conforms to necessary physical property limitations. A major advantage of the 8 vol% aromatic SAF blendstock is that it has the potential for being a drop-in fuel at blending levels well over 50% because of its aromatics content, although the low molecular

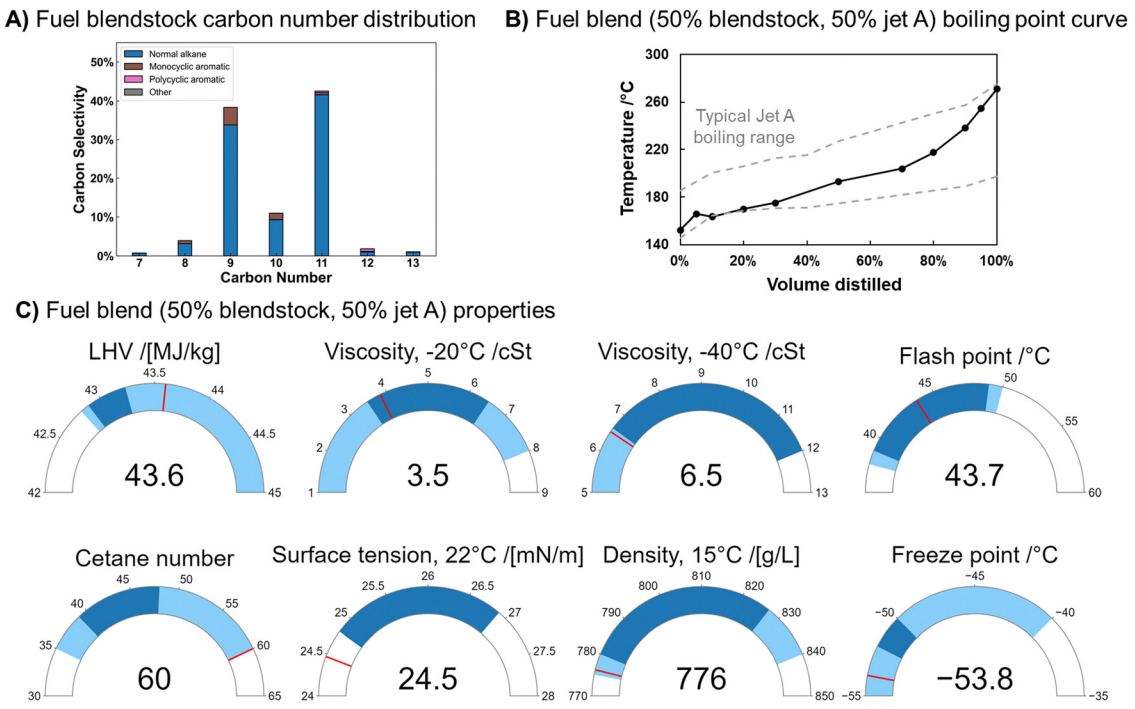

Fig. 7 Properties of SAF blendstock blended 50/50 (vol/vol) in Jet A. (A) SAF (92% alkane mixture, 8% aromatics mixture) contents; (B) boiling point curve of SAF blend compared to typical Jet A boiling range from CRC World Fuel Sampling Program; (C) fuel properties of SAF blend (red lines and numbers) compared to ASTM D7566 standard ranges (baby blue regions; cetane number is D4054 required range) and typical Jet A ranges (dark blue regions). LHV = lower heating value. There is currently no ASTM standard for surface tension.

diversity of this specific blendstock would likely preclude it from use as a drop-in SAF. Currently there is no approval pathway for blends above 50% but it is anticipated that a pathway for approval of 100% drop-in SAF will be established within the next few years. In the study reported here property measurements were limited by available sample volumes. Considerable additional property measurements and combustion rig testing would be required for full approval of VFA-derived SAF as a blend component or a neat fuel.

Technoeconomic analysis, life cycle assessment, and environmental justice metrics

A summary of the TEA and LCA results is provided in Table 1. The LCA indicated a highly favorable fuel carbon intensity (−151 g CO_2eq per MJ, a 268% reduction compared to petroleum jet fuel), driven primarily by significant credits associated with diverting food waste from landfills. This result is generally in line with those from our previous work[7,10] and is in fact more favorable due to lower fuel yields; the GHG avoidance credits are distributed across a lower volume of fuel, decreasing (making more negative) the carbon intensity per fuel volume. This favorable fuel carbon intensity enables significant revenues from policy incentives, resulting in an MJSP of $2.30 per gal. Comparing this value to the average market value of petroleum jet fuel ($1.76 per gal, based on a 7-year average of published prices[65]) indicates that the proposed process could be economically competitive when including these policy incentives. Economics were shown to be more challenging without incentives, with a resulting MJSP of $9.86 per gal.

A cost breakdown of the process (Fig. S9, ESI†) indicates that the MJSP was largely driven by the capital investment and fixed costs, while variable operating costs were less significant. The VFA upgrading operations were associated with the most capital cost (51%) followed by anaerobic digestion (37%) and VFA separation (10%). Key variable costs included the sulfolane solvent used in the BTEX separations (34% of variable operating costs), hydrogen used in HDO (24% of variable operating costs) and purchased electricity (32% of variable operation costs).

One challenge commonly encountered in biofuel production is achieving high carbon yields from biomass to fuels and products. Significant losses during biochemical conversion, especially using a heterogeneous feedstock such as food waste, are not uncommon; in the case of this process, the carbon yield to VFAs after arrested anaerobic digestion and recovery is 23%. Because of these losses, it is important to minimize additional losses during upgrading. The heavier VFAs (Fig. 6C, primarily C_{4-6}), upgraded through ketonization and subsequent HDO, achieve this well, with a 91% carbon yield to product (SAF). However, there are significantly higher losses for the lighter VFAs (Fig. 6B, primarily C_{2-4}) which are upgraded by ketonization and subsequent cyclization, with a 49% carbon yield to products (SAF, BTEX, and naphtha). While some of this carbon is lost in ketonization (14% of upgrading losses), the bulk of it is lost as light gases from the cyclization reaction (37%). Although the cyclization approach results in the production of sustainable BTEX and demonstrates improved potential for scalability compared to alternatives considered previously,[66] these losses are a significant challenge for achieving improved economics. We are currently investigating upgrading approaches which maximize carbon efficiency to fuels and products while minimizing the production of less-valuable light gases.

Given the uncertainty associated with this feasibility-level TEA, a single-point sensitivity analysis was performed on key economic and process variables. Each variable was varied over a range representing alternative scenarios. Fig. S10 (ESI†) shows the variables considered, their respective ranges, and the resultant impact on the MJSP. The cost of the food waste feedstock had the most significant impact and was varied from −$50 per wet ton (representing an optimistic cost available in select areas, as reported in Badgett, Newes, and Milbrandt[67]) to $76 per wet ton (representing near term average prices in the 2023 Billion Ton Report[68]). This range had significant implications on process economics, with the optimistic value resulting in a highly negative MJSP (−$5.23 per gal, an improvement of $7.23 compared to the base case) and the more conservative value increasing the MJSP to $13.75 per gal (an increase of $11.45 per gal compared to the base case).

Other variables also had significant impacts on the MJSP, though none as large as the food waste cost. Given some uncertainty in the capital costs for this feasibility-level analysis, we varied the total capital investment by ±50%, resulting in a MJSP variation of ±$2.42 per gal. Economics were also sensitive to variables related to the policy incentives; when the CI credit associated with diverting food waste from landfills was eliminated, the MJSP increased by $3.21 per gal. Although this is significant, it should be noted that the process still satisfied the 50% GHG emission reduction threshold without the credit and thus qualified for all policy incentives. Conversely, increasing the CI credit by 50% resulted in an MJSP reduction of $1.56. Policy credit values also influenced process economics; when varied by ±50%, the MJSP varied by $2.17 per gal and $0.72 per gal for LCFS and RIN credits, respectively. The price of the BTEX and naphtha coproducts had less significant impacts on the MJSP, resulting in variation of less than $0.30 per gal when varied over the ranges considered.

Table 1 Summary of TEA and LCA results for the conversion of food waste to fuels and chemicals

Description	Value
MJSP with policy incentives ($ per gal Jet)	$2.30
MJSP without policy incentives ($ per gal jet)	$9.87
Total fuel yield (gal jet per dry ton)	26.55
Fuel carbon intensity (g CO_{2eq} per MJ)	−151
Fixed capital investment	$19 096 000
Variable operating costs ($ per year)	$375 000
Fixed operating costs ($ per year)	$1 911 000
Revenue ($ per year)	$5 634 000
SAF (@$1.76 per gal)	18%
Naphtha	2%
BTEX	2%
Policy credits	77%

Table S13 (ESI†) contains a full accounting of the JUST-R metrics, accounting for environmental justice aspects of our research and envisioned process implementation. Most metrics for the research are positive, although the metrics do expose several weaknesses and blind spots (*e.g.* stakeholder communication, diversity of audiences reached, identification of set *vs.* flexible parameters, and air pollution) which can be addressed with further research.

Conclusion

We have demonstrated in this work a wholly continuous catalytic process for converting wet waste-derived VFAs to sustainable aviation fuel blendstocks and platform chemicals, with conversion of light (C_{3-7}) ketones over H/ZSM-5 to a mixture of hydrocarbons without addition of external H_2 as a major process addition. Alkanes coming from C_{5-7} VFAs mixed with aromatics coming from C_{2-4} VFAs are shown to comprise a viable SAF blendstock capable of being mixed with an equal amount of Jet A and meeting all basic aviation fuel requirements. When this process is applied to the conversion of VFAs derived from food waste, significant GHG reductions can be demonstrated (−268% compared to conventional jet fuel) and projected economics are competitive with petroleum jet with the inclusion of currently active policy incentives.

Author contributions

JHM: conceptualization, methodology, investigation, data curation, writing – original draft, writing – review & editing, visualization, supervision, funding acquisition; MA: investigation, data curation; JS: investigation, resources; AJK: investigation, writing – review & editing; MRW: formal analysis, writing – original draft. writing – review & editing; RLM: conceptualization, methodology, writing – original draft, writing – review & editing; GF: methodology, investigation, resources, writing – original draft; JL: investigation; CP: investigation, writing – original draft, MAT: methodology, investigation, writing – original draft.

Data availability

The data supporting this article have been included as part of the ESI.†

Conflicts of interest

There are no conflicts to declare.

Acknowledgements

We thank Dr Claire T. Nimlos and Gabrielle Kliegle for materials characterization assistance and Drs Randy Cortright (NREL) and Bruce Adkins (Oak Ridge National Lab) for guiding advice. We would also like to thank Jeroen van Dorp, Robbert Binneveld, and Maurice Oltheten (ChainCraft) for supplying ChainCraft salts and background information. This research was conducted as part of the ChemCatBio Consortium Catalytic Upgrading of Biochemical Intermediates project sponsored by the US Department of Energy – Office of Energy Efficiency and Renewable Energy, Bioenergy Technologies Office. Work at the National Renewable Energy Laboratory was performed under Contract DE347AC36-99GO10337. The views expressed in the article do not necessarily represent the views of the U.S. Department of Energy or the U.S. Government. The U.S. Government retains and the publisher, by accepting the article for publication, acknowledges that the U.S. Government retains a nonexclusive, paid-up, irrevocable, worldwide license to publish or reproduce the published form of this work, or allow others to do so, for U.S. Government purposes.

References

1 IPCC, AR6 Synthesis Report: Climate Change 2023 – IPCC.
2 DOE Launches New Energy Earthshot to Decarbonize Transportation and Industrial Sectors, **https://www.energy.gov/articles/doe-launches-new-energy-earthshot-decarbonize-transportation-and-industrial-sectors**, (accessed June 18, 2023).
3 R. Dalke, D. Demro, Y. Khalid, H. Wu and M. Urgun-Demirtas, *Renewable Sustainable Energy Rev.*, 2021, **151**, 111554.
4 A. H. Bhatt, Z. (Jason) Ren and L. Tao, *iScience*, 2020, 101221.
5 M. T. Holtzapple, H. Wu, P. J. Weimer, R. Dalke, C. B. Granda, J. Mai and M. Urgun-Demirtas, *Bioresour. Technol.*, 2022, **344**, 126253.
6 H. Wu, T. Scheve, R. Dalke, M. Holtzapple and M. Urgun-Demirtas, *Chem. Eng. J.*, 2023, **459**, 140080.
7 N. A. Huq, G. R. Hafenstine, X. Huo, H. Nguyen, S. M. Tifft, D. R. Conklin, D. Stück, J. Stunkel, Z. Yang, J. S. Heyne, M. R. Wiatrowski, Y. Zhang, L. Tao, J. Zhu, C. S. McEnally, E. D. Christensen, C. Hays, K. M. van Allsburg, K. A. Unocic, H. M. Meyer, Z. Abdullah and D. R. Vardon, *Proc. Natl. Acad. Sci. U. S. A.*, 2021, **118**, e2023008118.
8 R. L. Skaggs, A. M. Coleman, T. E. Seiple and A. R. Milbrandt, *Renewable Sustainable Energy Rev.*, 2018, **82**, 2640–2651.
9 US EPA, Importance of Methane, **https://www.epa.gov/gmi/importance-methane**, (accessed September 16, 2022).
10 J. H. Miller, S. M. Tifft, M. R. Wiatrowski, P. T. Benavides, N. A. Huq, E. D. Christensen, T. Alleman, C. Hays, J. Luecke, C. M. Kneucker, S. J. Haugen, V. Sànchez i Nogué, E. M. Karp, T. R. Hawkins, A. Singh and D. R. Vardon, *iScience*, 2022, **25**, 105384.
11 Grand View Research, Petrochemicals Industry Outlook Data Book, 2023–2030, Grand View Research.
12 J. Sun, S. Shao, X. Hu, X. Li and H. Zhang, *ACS Sustainable Chem. Eng.*, 2022, **10**, 11030–11040.
13 S. Luo and J. L. Falconer, *J. Catal.*, 1999, **185**, 393–407.
14 B. Oliver-Tomas, M. Renz and A. Corma, *J. Mol. Catal. A: Chem.*, 2016, **415**, 1–8.

15 M. Balakrishnan, E. R. Sacia, S. Sreekumar, G. Gunbas, A. A. Gokhale, C. D. Scown, F. D. Toste and A. T. Bell, *Proc. Natl. Acad. Sci. U. S. A.*, 2015, **112**, 7645–7649.
16 E. R. Sacia, M. Balakrishnan, M. H. Deaner, K. A. Goulas, F. D. Toste and A. T. Bell, *ChemSusChem*, 2015, **8**, 1726–1736.
17 B. Rozmysłowicz, J. Hau Yeap, A. M. I. Elkhaiary, M. T. Amiri, R. L. Shahab, Y. M. Questell-Santiago, C. Xiros, B. P. L. Monnier, M. H. Studer and J. S. Luterbacher, *Green Chem.*, 2019, **21**, 2801–2809.
18 D. Salvachúa, P. O. Saboe, R. S. Nelson, C. Singer, I. McNamara, C. del Cerro, Y.-C. Chou, A. Mohagheghi, D. J. Peterson, S. Haugen, N. S. Cleveland, H. R. Monroe, M. T. Guarnieri, E. C. D. Tan, G. T. Beckham, E. M. Karp and J. G. Linger, *Cell Rep. Phys. Sci.*, 2021, **2**, 100587.
19 P. O. Saboe, L. P. Manker, H. R. Monroe, W. E. Michener, S. Haugen, E. C. D. Tan, R. L. Prestangen, G. T. Beckham and E. M. Karp, *Green Chem.*, 2021, **23**, 4386–4402.
20 P. O. Saboe, L. P. Manker, W. E. Michener, D. J. Peterson, D. G. Brandner, S. P. Deutch, M. Kumar, R. M. Cywar, G. T. Beckham and E. M. Karp, *Green Chem.*, 2018, **20**, 1791–1804.
21 J. Cao, S. Ding, H. Wang, J. Han, Q. Ge and X. Zhu, *Ind. Eng. Chem. Res.*, 2019, **58**, 10307–10316.
22 R. D. Cortright and P. G. Blommel, US8017818B2, 2008, p. 67.
23 J. Fuhse and F. Bandermann, *Chem. Eng. Technol.*, 1987, **10**, 323–329.
24 E. V. Fufachev, B. M. Weckhuysen and P. C. Bruijnincx, *Green Chem.*, 2020, **22**, 3229–3238.
25 X. Wang, S. Ding, H. Wang, X. Liu, J. Han, Q. Ge and X. Zhu, *Appl. Catal., A*, 2017, **545**, 79–89.
26 S. Taco-Vasquez and M. T. Holtzapple, *PLoS One*, 2022, **17**, e0277184.
27 D02 Committee, *ASTM D7566-24 "Standard Specification for Aviation Turbine Fuel Containing Synthesized Hydrocarbons,"* ASTM International, 2024.
28 J. H. Miller, G. R. Hafenstine, H. H. Nguyen and D. R. Vardon, *Ind. Eng. Chem. Res.*, 2022, **61**, 2997–3010.
29 X. Huo, N. A. Huq, J. Stunkel, N. S. Cleveland, A. K. Starace, A. E. Settle, A. M. York, R. S. Nelson, D. G. Brandner, L. Fouts, P. C. St John, E. D. Christensen, J. Luecke, J. H. Mack, C. S. McEnally, P. A. Cherry, L. D. Pfefferle, T. J. Strathmann, D. Salvachúa, S. Kim, R. L. McCormick, G. T. Beckham and D. R. Vardon, *Green Chem.*, 2019, **21**, 5813–5827.
30 D. E. Mears, *J. Catal.*, 1971, **20**, 127–131.
31 P. B. Weisz and C. D. Prater, in *Advances in Catalysis*, ed. W. G. Frankenburg, V. I. Komarewsky and E. K. Rideal, Academic Press, 1954, vol. 6, pp. 143–196.
32 D. J. Collins, R. J. Medina and B. H. Davis, *Can. J. Chem. Eng.*, 1983, **61**, 29–35.
33 S. Haag, M. Hanebuth, G. T. P. Mabande, A. Avhale, W. Schwieger and R. Dittmeyer, *Microporous Mesoporous Mater.*, 2006, **96**, 168–176.
34 Coordinating Research Council, *CRC Aviation Committee-World Fuel Sampling Program*, 2006.
35 M. Wiatrowski, J. H. Miller, A. H. Bhatt, S. M. Tifft, Z. Abdullah and L. Tao, *Renewable Energy*, 2024, In Review.
36 AspenTech, Aspen Plus V10 Aspen Technology, Inc., Bedford, MA, 2017.
37 G. Yadav, A. Singh, A. Dutta, T. Uekert, J. S. DesVeaux, S. R. Nicholson, E. C. D. Tan, C. Mukarakate, J. A. Schaidle, C. J. Wrasman, A. C. Carpenter, R. M. Baldwin, Y. Román-Leshkov and G. T. Beckham, *Energy Environ. Sci.*, 2023, **16**, 3638–3653.
38 D. Humbird, R. Davis, L. Tao, C. Kinchin, D. Hsu, A. Aden, P. Schoen, J. Lukas, B. Olthof, M. Worley, D. Sexton and D. Dudgeon, *Process Design and Economics for Biochemical Conversion of Lignocellulosic Biomass to Ethanol: Dilute-Acid Pretreatment and Enzymatic Hydrolysis of Corn Stover*, National Renewable Energy Lab. (NREL), Golden, CO, United States, 2011.
39 N. S. Dutta, E. Gill, B. K. Arkhurst, M. Hallisey, K. Fu and K. Anderson, *Joule*, 2023, **7**, 431–437.
40 S. Kramer, G. Andac, J. Heyne, J. Ellsworth, P. Herzig and K. C. Lewis, *Front. Energy Res*, 2022, **9**, 782823.
41 J. Holladay, Z. Abdullah and J. S. Heyne, *Sustainable Aviation Fuel: Review of Technical Pathways*, DOE/EE-2041 8292, USDOE Office of Energy Efficiency and Renewable Energy (EERE), Bioenergy Technologies Office (EE-3B) (Bioenergy Technologies Office Corporate), DOE EERE, 2020.
42 N. A. Bhore, M. T. Klein and K. B. Bischoff, *Ind. Eng. Chem. Res.*, 1990, **29**, 313–316.
43 N. A. Bhore, M. T. Klein and K. B. Bischoff, *Chem. Eng. Sci.*, 1990, **45**, 2109–2116.
44 D. Best and B. W. Wojciechowski, *J. Catal.*, 1977, **47**, 11–27.
45 T. M. John and B. W. Wojciechowski, *J. Catal.*, 1975, **37**, 240–250.
46 J. H. Miller and A. Bhan, *ChemCatChem*, 2018, **10**, 5242–5255.
47 L. Bui, R. Chakrabati and A. Bhan, *ACS Catal.*, 2016, **6**, 6567–6850.
48 L. Bui and A. Bhan, *Appl. Catal., A*, 2017, **546**, 87–95.
49 Y. K. Chow, N. F. Dummer, J. H. Carter, R. J. Meyer, R. D. Armstrong, C. Williams, G. Shaw, S. Yacob, M. M. Bhasin, D. J. Willock, S. H. Taylor and G. J. Hutchings, *ChemPhysChem*, 2018, **19**, 402–411.
50 H. Wei, C. Gomez, J. Liu, N. Guo, T. Wu, R. Lobo-Lapidus, C. L. Marshall, J. T. Miller and R. J. Meyer, *J. Catal.*, 2013, **298**, 18–26.
51 M. Cohen, T. Goculdas and D. G. Vlachos, *React. Chem. Eng.*, 2023, **8**, 824–837.
52 W. J. Movick, G.-N. Yun, I. Tyrone Ghampson and S. Ted Oyama, *J. Catal.*, 2021, **404**, 786–801.
53 B. L. Foley, B. A. Johnson and A. Bhan, *ACS Catal.*, 2019, **9**, 7065–7072.
54 N. K. Razdan, A. Kumar, B. L. Foley and A. Bhan, *J. Catal.*, 2020, **381**, 261–270.
55 A. Hwang and A. Bhan, *Acc. Chem. Res.*, 2019, **52**, 2647–2656.
56 S. Ilias and A. Bhan, *ACS Catal.*, 2013, **3**, 18–31.
57 T. C. Hoff, R. Thilakaratne, D. W. Gardner, R. C. Brown and J.-P. Tessonnier, *J. Phys. Chem. C*, 2016, **120**, 20103–20113.

58 B. Boekaerts and B. F. Sels, *Appl. Catal., B*, 2020, 119607.
59 T. N. Pham, D. Shi and D. E. Resasco, *Top. Catal.*, 2014, **57**, 706–714.
60 T. N. Pham, T. Sooknoi, S. P. Crossley and D. E. Resasco, *ACS Catal.*, 2013, **3**, 2456–2473.
61 H. Zhang, Y.-T. Cheng, T. P. Vispute, R. Xiao and G. W. Huber, *Energy Environ. Sci.*, 2011, **4**, 2297–2307.
62 D02 Committee, *D4054-23: Standard Practice for Evaluation of New Aviation Turbine Fuels and Fuel Additives*, ASTM International, 2023.
63 D. J. Cronin, S. Subramaniam, C. Brady, A. Cooper, Z. Yang, J. Heyne, C. Drennan, K. K. Ramasamy and M. R. Thorson, *Energies*, 2022, **15**, 1306.
64 D02 Committee, *ASTM D7566-24 "Standard Specification for Aviation Turbine Fuel Containing Synthesized Hydrocarbons,"* ASTM International, 2024.
65 Petroleum & Other Liquids Data – U.S. Energy Information Administration (EIA), **https://www.eia.gov/petroleum/data.php**, (accessed September 21, 2022).
66 R. Davis and A. Bartling, *Biochemical Conversion of Lignocellulosic Biomass to Hydrocarbon Fuels and Products: 2021 State of Technology and Future Research*, National Renewable Energy Laboratory, National Renewable Energy Laboratory, 2022.
67 A. Badgett, E. Newes and A. Milbrandt, *Energy*, 2019, **176**, 224–234.
68 M. H. Langholtz, *2023 Billion-Ton Report*, US Department of Energy, Oak Ridge National Laboratory, 2024.